RSC Advances

ROYAL SOCIETY OF CHEMISTRY

www.rsc.org/advances

Journal Name

RSCPublishing

ARTICLE

Using Halogen···Halogen Interactions or C/N–H···Cl Hydrogen Bonding to Direct Crystal Packing in Tetrachlorophthalic Acid with N–heterocyclic Compounds

Cite this: DOI: 10.1039/x0xx00000x

Received 00th January 2012,
Accepted 00th January 2012

DOI: 10.1039/x0xx00000x

www.rsc.org/

Yanjing Hu, Zhiqiang Li, Yiran Zhao, Yu Yang*, Faqian Liu,and Lei Wang*

In exploring the tetrachlorophthalic acid (H_2-tcpH) with a series of N–heterocyclic compounds, eight different types of supramolecular complexes have been obtained, namely, [(H-1,10-phen)·(H-tcpH)·(H_2-tcpH)·(CH_3OH)] (**1**), [(H-Hatz)·(H-tcpH)] (**2**), [(H_2-L5)·(H-tcpH)$_2$] (**3**), [(H-Hampym)·(H-tcpH)] (**4**), [(H_2-edm)·(H-tcpH)$_2$] (**5**), [(H-ahmp)$_2$·(tcpH)·2(H_2O)] (**6**), [(H_2-L7)·(tcpH)·2(H_2O)] (**7**), and [(H-Bim)·(H-tcpH)·(H_2O)] (**8**) (where 1,10-phen = 1,10-phenanthroline, Hatz = 3-amino-1,2,4-triazole, L5 = 1,4-bis[(2-methylimidazole-1-yl)methyl]benzene, Hampym = 2-aminopyrimidine, edm = ethylenediamine, ahmp = 2-amino-4-hydroxy-6-methylpyrimidine, L7 = 1,2-bis[(2-methylimidazole-1-yl)methyl]benzene, Bim = benzimidazole). In these eight complexes, they displayed the amusing structural characteristics and a vast of hydrogen bonding. Of this, crystals **1**–**5** generated a 3D supramolecular structure through Cl···Cl interactions, whilst the C–H···Cl and N–H···Cl hydrogen bonding existed in the 3D construction of complexes **6**–**8**. In addition, all the complexes were fully characterized by single crystal X-ray diffraction analysis, elemental analysis, infrared spectroscopy (IR), and thermogravimetric analysis (TGA).

Introduction

Non-covalent interactions, such as hydrogen bonding, π–π interactions, van der Waals forces, and other weak interactions[1] are responsible for the construction of supramolecular architectures in the solid-state materials. In the past few years, tremendous efforts have been made to explore the new types of intermolecular interactions to synthesis multi-component supramolecules.[2] In particular, halogen bonding has grown from a scientific curiosity to one of the most intriguing non-covalent interactions in chemists' eyes.[3] The term "halogen bonding" (XB) refers to any non-covalent interaction involving halogens as acceptors of electron density.[4]

Key Laboratory of Eco-chemical Engineering, Ministry of Education, State Laboratory of Inorganic Synthesis and Applied Chemistry, College of Chemistry and Molecular Engineering, Qingdao University of Science and Technology, Qingdao 266042, P. R. China. E-mail: inorchemwl@126.com; yangyu9039@163.com; Fax: (+86) 532-840-22681

† Electronic Supplementary Information (ESI) available: IR, TGA, DSC data and synthons XXV–XXXIV about this work. CCDC reference numbers 1032979-1032986. For ESI and crystallographic data in CIF or other electronic format see DOI: XXXXXXX

Allen and co-workers have been showed that the XB manifests as a directional attractive interaction through the statistical analysis, which based on intermolecular contract distances shorter than 1.26 times the sum of the van der Waals radii of two interacting atoms.[5] Halogen···halogen interactions and C/N–H···halogen interactions are one of the most important parts of non-covalent interactions.[6] Such Halogen···halogen interactions have been termed as Type I ($\theta_1 \approx \theta_2$) and Type II ($\theta_1 \approx 180°$, $\theta_2 \approx 90°$) depending on the angular approach of the halogens toward each other (**Scheme 1**). In many molecular crystals without the strong hydrogen bonding (O/N–H···O and O/N–H···N), the X···X and C/N–H···X interactions dominate the molecular arrangement as an effective directional tool.[7] For example, the presence of C–H···O/Cl, C=O···Cl, and Cl···Cl

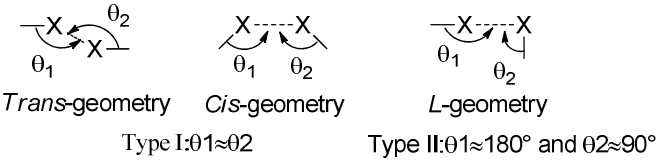

Scheme 1. Geometrical Classification of Halogen···Halogen Interaction as Type I and Type II.

interactions in two concomitant conformational polymorphs of 1,3,5-tris(4-chlorobenzoyl) benzene have been communicated by Pigge and co-workers.[8] In addition, the Jin group first prepared a novel organic phosphorescent co-crystal from 1,4-diiodotrafluorobenzene and carbazole using a C–I···π XB and they based on the C–I···N XB and π–hole···F bonds.[4e,9]

In fact, up to present, rationally controlling the desired structures of solid-state materials still remains a great challenge.[10] For this, as Desiraju pointed out, crystal structures are not related to molecular structures (functional groups) in simple way: the molecules come to crystal structures which is an emergent property.[11] Fortunately, supramolecular synthons appeared.[12] Supramolecular synthons are structural units of a supramolecule which are assembled *via* intermolecular forces.[13] In a paper by Khavasi and Tehrani, Br···Br and N···Br halogen bonding synthons have been displayed in the N-(3-bromophenyl)-2-pyrazinecarboxamide molecules.[14] Synthons $R^2_2(6)$ and $R^1_2(5)$ are formed between neighboring 2,4,6,8,10,12-hexanitrohexaazaisowurtzitane (CL-20) molecules and between CL-20 and conformer molecules in a paper which is composed by Zhang and co-workers in 2014.[15] Supramolecular synthon is a simple and popular way to understand the intermolecular interactions.[15,16] The identification of useful supramolecular synthons is an important aspect of current crystal engineering strategies and it is helpful in the design of materials with predetermined properties.[15,17]

The carboxylic acids are capable of functioning as hydrogen bonding donors and/or acceptors resulting in supramolecular frameworks by intermolecular interactions and the carboxylic acids aggregate in solid state as dimer, catemer, and bridged motifs,[18] so they are frequently chosen as building blocks for crystal engineering.[19] Furthermore, halogenated compounds have received widespread attention due to their application in life science.[6b,20] In view of the above mentioned interests, we select tetrachlorophthalic acid (H_2-tcpH) to explore the nature of intermolecular interactions with a series of N–heterocyclic compounds to continue of our work in organic crystals.[21]

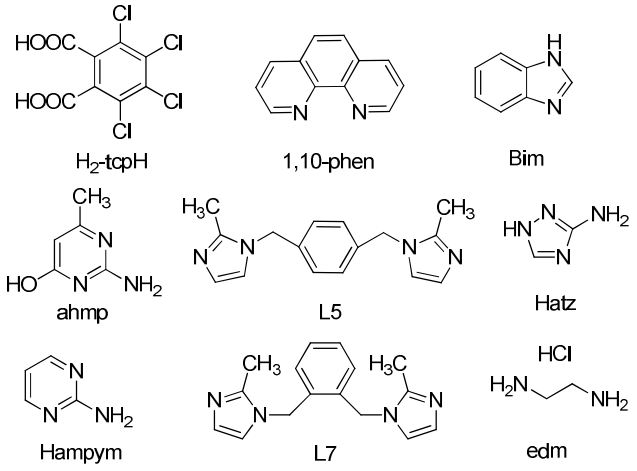

Scheme 2. Molecular Structures in This Work.

Herein, we report the synthesis and the crystal structures of eight crystals, namely, [(H-1,10-phen)·(H-tcpH)·(H_2-tcpH)·(CH_3OH)] (**1**), [(H-Hatz)·(H-tcpH)] (**2**), [(H_2-L5)·(H-tcpH)$_2$] (**3**), [(H-Hampym)·(H-tcpH)] (**4**), [(H_2-edm)·(H-tcpH)$_2$] (**5**), [(H-ahmp)$_2$·(tcpH)·2(H_2O)] (**6**), [(H_2-L7)·(tcpH)·2(H_2O)] (**7**), and [(H-Bim)·(H-tcpH)·(H_2O)] (**8**) (**Scheme 2**).

Experimental

Starting Materials. All chemicals and solvents used for synthesis were obtained from commercial sources and were used as received, without further purification, except the ligands L5 and L7. They were prepared by the procedure given in the literatures.[22]

Physical Measurements. Infrared spectra were recorded with a Nicolet Impact 410 FTIR spectrometer in the range of 4000-400 cm^{-1}, and samples were prepared as KBr pellets. Absorptions are denoted as follows: strong (s), medium (m), and weak (w) in the synthesis section. Carbon, hydrogen, and nitrogen contents were performed with a Perkin–Elmer 2400 elemental analyzer. Thermogravimetric analysis (TGA) was performed from room temperature to 900℃ by using a Perkin-Elmer TGA–7 TG analyzer with a heating rate of 10℃/min in a N_2 atmosphere.

General Procedures for the Preparation of Single Crystals.

Synthesis of [($C_{12}H_9N_2^+$)·($C_8HO_4Cl_4^-$)·($C_8H_2O_4Cl_4$)·(CH_3OH)] (1) A solution of 1,10-phen (99 mg, 0.05 mmol) in 5 mL of distilled water was mixed with H_2-tcpH (31.8 mg 0.10 mmol) in 5 mL of methanol. The reaction mixture was stirred for 15 min and a clear homogeneous solution was obtained. Then the solution was allowed to stand at room temperature for slow evaporation. Colorless, block crystals were gained after two weeks. The obtained crystals were separated from the mother solution by filtration, washed with a methanol–distilled water solution (v/v = 1 : 1), and dried under vacuum. Yield: 64%. Anal. calcd for $C_{29}H_{16}Cl_8N_2O_9$: C, 42.44; H, 1.95; N, 3.41%. Found: C, 44.92; H, 2.07; N, 3.06%. Infrared spectrum (KBr disc, cm^{-1}): 3450s, 3102s, 2920s, 2584s, 1757w, 1615m, 1563m, 1511s, 1471s, 1433s, 1343m, 1265w, 1123m, 1045m, 916m, 851w, 811s, 773m, 721m, 683m, 657m, 617m, 591m, 451s, 476m, 398m.

Synthesis of [($C_2H_5N_4^+$)·($C_8HO_4Cl_4^-$)] (2). To a tetrahydrofuran–distilled water solution (v/v = 1 : 1, 10 mL) containing Hatz (16.8 mg, 0.20 mmol) was added H_2-tcpH (31.8 mg, 0.10 mmol) with constant stirring for 15 min. The clear and homogeneous solution was slowly evaporated at room temperature, and block colorless crystals were obtained three weeks later. The crystals were picked up from the mother liquor and washed with tetrahydrofuran–distilled water solution (v/v = 1 : 1), and dried under vacuum. Yield: 67%. Anal. calcd for $C_{10}H_6Cl_4N_4O_4$: C, 30.93; H, 1.55; N, 14.43%. Found: C, 32.04; H, 1.87; N, 14.06%. Infrared spectrum (KBr disc, cm^{-1}): 3430w, 3258w, 3161m, 2946m, 2733m, 2566m, 1913s, 1692w, 1576w, 1561w, 1543w, 1427m, 1408m, 1344w, 1244w, 1202w, 1137s, 1120m, 1055s, 1008s, 956m, 932s, 904m, 865m, 839s, 824s, 795s, 756s.

Synthesis of [($C_{16}H_{20}N_4^{2+}$)·($C_8HO_4Cl_4^-$)$_2$] (3).

A mixture of L5 (15.1 mg, 0.05 mmol), H_2-tcpH (31.8 mg, 0.10 mmol), $Ni(NO_3)_2$ (29.8 mg, 0.01mmol), NMP (5 mL), and distilled water (5 mL) was sealed in a Teflon-lined stainless steel vessel (15 mL), which was heated at 120 °C for three days and cooled to room temperature at a rate of 5 °C/h. Colorless, block shaped crystals of **3** were collected in 38% yield. Anal. calcd for $C_{32}H_{22}Cl_8N_4O_8$: C, 43.93; H, 2.52; N, 6.41%. Found: C, 44.42; H, 2.66; N, 7.52%. Infrared spectrum (KBr disc, cm^{-1}): 3395w, 3127m, 2991s, 2634s, 2455s, 1946s, 1633w, 1600w, 1526w, 1429w,1448w, 1338w, 1289m, 1230m, 1195m, 1142m, 1120m, 1049m, 979s, 924m, 905m, 843m, 795w, 742w, 651m, 616m, 570m, 465m, 428m.

Synthesis of $[(C_4H_6N_3^+)\cdot(C_8HO_4Cl_4^-)]$ (4).

5 mL of a distilled water solution of Hampym (9.5 mg, 0.10 mmol) was mixed with 5 mL of an ethanol solution of H_2-tcpH (31.8 mg, 0.10 mmol), and the colorless solution was stirred for 15 min and kept for slow evaporation at room temperature. Colorless block shaped crystals in about an 80% yield were obtained after three weeks and separated from the mother liquor. The crystals were washed with an ethanol–distilled water solution (v/v = 1 : 1) and dried under vacuum. Anal. calcd for $C_{12}H_7Cl_4N_3O_4$: C, 36.10; H, 1.75; N, 10.53%. Found: C, 37.88; H, 1.84; N, 10.48%. Infrared spectrum (KBr disc, cm^{-1}): 3415m, 3323m, 3218s, 3131s, 3092s, 2961s, 2891s, 2836s, 2789m, 2737m, 2686m, 1907s, 1694w, 1682w, 1655w, 1542w, 1459m, 1414w, 1344w, 1287m, 1226w, 1067m, 990m, 898m, 872s, 797w, 742w, 720m, 666w, 638w, 603w, 577m, 541m, 479s, 437m, 423m.

Synthesis of $[C_2H_{10}N_2^{2+})\cdot(C_8HO_4Cl_4^-)_2]$ (5).

A solution of H_2-tcpH (31.8 mg, 0.10 mmol) was prepared in 5 mL of acetone. 5 mL of a distilled water solution of edm (4.9 mg, 0.05 mmol) was added to the above solution. The resulting solution was stirred for 15 min and kept at room temperature for crystallization. Colorless, block crystals were gained after two weeks. The obtained crystals were separated from the mother solution by filtration, washed with a acetone–distilled water solution (v/v = 1 : 1), and dried under vacuum. Yield: 68%. Anal. calcd for $C_9H_6Cl_4NO_4$: C, 32.34; H, 1.80; N, 4.19%. Found: C, 34.01; H, 1.98; N, 4.68%. Infrared spectrum (KBr disc, cm^{-1}): 3436s, 3174m, 3031m, 2944m, 2616s, 2459s, 1716w, 1571w, 1532w, 1478s, 1414s, 1343w, 1239w, 1198m, 1125m, 1037s, 1011s, 933s, 902s, 670m, 648m, 605s, 456s, 415s.

Synthesis of $[(C_5H_8ON_3^+)_2\cdot(C_8O_4Cl_4^{2-})\cdot 2(H_2O)]$ (6).

H_2-tcpH (31.8 mg, 0.10 mmol) and ahmp (25.0 mg, 0.20 mmol) were taken in a 1 : 2 molar ratio and dissolved in an ethanol–distilled water solution (v/v = 1 : 1 10 mL), the solution was stirred for 15 min until a colorless solution was obtained. Good quality crystals, suitable for diffraction, were gained after one week as the solution evaporated slowly at room temperature. The obtained crystals were separated from the mother liquor by filtration, washed with the ethanol–distilled water solution (v/v = 1 : 1), and dried in a vacuum desiccator. Yield: 62%. Anal. calcd for $C_{18}H_{20}Cl_4N_6O_8$: C, 36.60; H, 3.39; N, 14.23%. Found: C, 36.88; H, 3.64; N, 15.45%. Infrared spectrum (KBr disc, cm^{-1}): 3408w, 3133m, 2756m, 1706w, 1686w, 1631w, 1591w, 1533w, 1479m, 1416w, 1370m, 1342w, 1250m, 1190s, 1127s, 1086m, 1045s, 951m, 911s, 840m, 669m, 649m, 619m, 582w, 539w, 508m.

Synthesis of $[(C_{16}H_{20}N_4^{2+})\cdot(C_8O_4Cl_4^{2-})\cdot 2(H_2O)]$ (7).

The same synthetic procedure as that for **6** was used except that ahmp was replaced by L7, affording colorless block crystals of **7** in 62% yield. Anal. calcd for $C_{24}H_{24}Cl_4N_4O_8$: C, 47.50; H, 3.96; N, 9.24%. Found: C, 49.42; H, 4.05; N, 10.20%. Infrared spectrum (KBr disc, cm^{-1}): 3481w, 3363w, 3138m, 3042m, 2974s, 2528s, 1967s, 1647w, 1602w, 1531m, 1457m, 1412m, 1381w, 1361w, 1339w, 1303m, 1250m, 1176m, 1156m, 1126s, 1092s, 1047s, 970s, 933m, 910m, 782m, 739m, 684m, 655w, 618m, 595m, 539m, 421s.

Table 1. Crystallographic Information of compounds 1-8

Compound	1	2	3	4	5	6	7	8
Empirical formula	$C_{29}H_{16}Cl_8N_2O_9$	$C_{10}H_6Cl_4N_4O_4$	$C_{32}H_{22}Cl_8N_4O_8$	$C_{12}H_7Cl_4N_3O_4$	$C_9H_6Cl_4NO_4$	$C_{18}H_{20}Cl_4N_6O_8$	$C_{24}H_{24}Cl_4N_4O_8$	$C_{15}H_{10}Cl_4N_2O_5$
M	820.04	387.99	874.14	399.01	333.95	590.20	606.27	440.05
Crystal system	monoclinic	orthorhombic	triclinic	monoclinic	monoclinic	triclinic	monoclinic	triclinic
Space group	$P2_1/n$	$Pbca$	$P\bar{1}$	$P2_1/c$	$C2/c$	$P\bar{1}$	$C2/c$	$P\bar{1}$
a/Å	18.1486(4)	9.4206(3)	8.5055(6)	12.614(3)	36.8502(17)	7.4149(4)	12.6127(5)	7.047(4)
b/Å	8.7692(2)	12.0251(3)	9.8663(7)	11.255(2)	5.5385(2)	8.9129(6)	23.7989(9)	8.497(5)
c/Å	22.0638(5)	24.0488(9)	11.0901(7)	10.900(2)	12.5520(6)	18.7130(11)	9.5324(4)	15.269(9)
α/°	90	90	88.177 (1)	90	90	97.470(5)	90	84.240(9)
β/°	111.758(2)	90	73.768(1)	106.969(3)	105.115(6)	97.712(5)	98.590(4)	83.995(10)
γ/°	90	90	87.108(1)	90	90	98.484(5)	90	72.863(9)
V/ Å^3	3261.26(13)	2724.34(15)	892.27(11)	1480.1(5)	2473.2(2)	1197.87(13)	2829.23(19)	866.5(9)
Z	4	8	1	4	8	2	4	2
T/K	293	293	293	293	293	293	293	293
D_c/g cm^{-3}	1.670	1.892	1.627	1.791	1.794	1.636	1.423	1.687
μ/mm^{-1}	0.748	0.892	0.689	0.822	0.960	0.552	0.463	0.714
F(000)	1648.0	1552.0	442.0	800.0	1336.0	604.0	1248.0	444.0
h, k, lmax	22,10,27	12,15,30	10,11,13	14,13,12	46,7,16	8,10,22	15,29,11	8,10,18
R_1[a]	0.0383	0.0306	0.0653	0.0554	0.0337	0.0497	0.0607	0.0891
wR_2[a](all data)	0.0991	0.0705	0.1787	0.1498	0.0897	0.1262	0.1551	0.2354
S(GOF on F^2)	1.043	1.055	1.043	1.077	1.041	0.977	1.039	0.951

[a] $R_1=\Sigma\Delta F_o\Delta-\Delta F_c\Delta/\Sigma\Delta F_o\Delta$. [b] $wR_2=[\Sigma w(F_o^2-F_c^2)^2/\Sigma w(F_o^2)^2]^{1/2}$.

Table 2. Intermolecular Interactions of 1–8

D-H···A (Å) (symmetry code)	D-H(Å)	H···A(Å)	D···A(Å)	∠D-H···A (deg)
1O3–H3···O7 (x,-1+y,z)	0.820	1. 753	2.571	175.0
O6–H6···O2 (–x,1–y,–z)	0.820	1.772	2.585	171.1
N2–H2···O9 (x,-1+y,z)	0.854	1.939	2.721	151.5
O9–H9···O5 (x,-1+y,z)	0.887	1.949	2.798	159.7
C36–H36···O4 (x,2-y,z)	0.930	2.568	3.491	171.8
2O3–H3···O2 (-1-x,-1-y,-z)	0.820	1.778	2.586	168.0
N4–H4···O1 (-1-x,-1-y,-z)	0.860	1.898	2.714	157.8
N1–H1B···N2 (-x,-y,-z)	0.860	2.233	3.058	160.5
N3–H3A···O2 (x,y,-1+z)	0.860	2.336	2.933	126.8
3O1–H1···O1 (x,y,z)	1.237	1.237	2.245	180.0
N2–H2···O4 (1+x,y,2+z)	0.860	2.025	2.763	143.4
C21–H21A···O3 (1+x,2+y,2+z)	0.970	2.420	3.218	139.2
4O8–H8···O2 (1–x,–y,–z)	0.818	1.667	2.483	174.4
O3–H3···O5 (-1+x,y,z)	0.823	1.691	2.490	163.2
N5–H5···O6 (2-x,2-y,-z)	0.860	1.829	2.640	156.5
N3–H3A···O1 (1-x,-y,-z)	0.859	1.835	2.649	157.5
C38–H38···O7 (-1+x,y,z)	0.930	2.617	3.256	126.4
C35–H35···O4 (-1+x,y,z)	0.930	2.629	3.270	126.6
5O4–H4···O1 (x,–1+y,z)	0.820	1.763	2.560	163.4
N1–H1A···O2 (x,–2+y,z)	0.890	1.900	2.743	157.2
N1–H1B···O2 (x,2+y,z)	0.890	1.969	2.847	168.5
N1–H1C···O1 (x,-1+y,z)	0.890	1.989	2.819	154.6
6N1–H1···O2 (x,y,z)	0.860	1.763	2.622	176.4
O7–H7B···O6 (x,y,z)	0.855	1.883	2.701	159.8
N4–H4···O4 (x,y,z)	0.860	1.884	2.668	150.9
N2–H2···O7 (x,y,-1+z)	0.860	1.888	2.747	177.0
O6–H6C···O3 (x,y,z)	0.850	1.904	2.743	168.7
O7–H7A···O8 (x,-1+y,z)	0.850	1.921	2.693	150.4
N5–H5···O1 (x,y,z)	0.860	1.938	2.774	163.7
O6–H6D···O5 (x,1+y,z)	0.850	1.950	2.783	166.1
N6–H6B···Cl4 (-1+x,y,z)	0.860	1.991	3.399	122.1
7N1–H1···O1 (-1+x,y,-1+z)	0.928	1.740	2.658	169.3
O3–H3B···O2 (-1+x,y,z)	0.850	1.904	2.753	176.8
O3–H3A···O1 (x,y,z)	0.850	2.032	2.872	169.3
C15–H15···Cl2 (-1+x,y,z)	0.930	3.118	4.017	163.0
8O3–H3···O2 (x,y,1+z)	0.820	1.779	2.568	160.8
N1–H1···O1 (2+x,y,z)	0.860	1.831	2.684	170.7
N2–H2···O5 (x,y,z)	0.860	1.838	2.666	161.1
O5–H5A···O2 (-1+x,y,z)	0.850	1.985	2.799	160.1
O5–H5B···O1 (x,y,z)	0.850	2.475	3.108	131.9
C19–H19···Cl2 (x,y,z)	0.930	2.933	3.640	133.9

Table 3. Halogen···Halogen Short Contact

Crystal	C–X···Y–C	X···Y(Å)	∠C–X···Y(°)	∠C–Y···X(°)	Summetry code	Type
1	C7–Cl6···Cl5–C14	3.513	161.1	122.0	(0.5-x,-0.5+y,0.5-z)/(1+x,y,z)	II
2	C6–Cl4···Cl3–C11	3.280	77.7	172.4	(-x,0.5+y,0.5-z)/(0.5+x,1+y,0.5-z)	II
	C73–Cl2···Cl1–C7	3.280	98.2	144.7	(-x,-1-y,-z)/(x,-0.5-y,-0.5+z)	II
3	C11–Cl2···Cl4–C15	3.399	165.8	123.4	(-1+x,y,z)/(1-x,3-y,1-z)	II
4	C31–Cl4···Cl3–C18	3.372	156.9	95.0	(1-x,1-y,-z)/(1-x,1-y,-z)	II
	C5–Cl5···Cl8–C32	3.373	94.4	157.0	(1-x,2-y,-z)/(1-x,3-y,-z)	II
5	C12–Cl2···Cl2–C12	3.707	126.8	126.8	(0.5-x,1.5-y,1-z)/(0.5+x,1.5-y,0.5+z)	I
	C11–Cl3···Cl4–C15	3.632	122.1	175.4	(0.5-x,-0.5+y,0.5-z)/(0.5+x,1.5-y,0.5+z)	II

Synthesis of $[(C_7H_7N_2^+)\cdot(C_8HO_4Cl_4^-)\cdot H_2O]$ (8).
Bim (11.8 mg, 0.10 mmol) was dissolved in 5 mL of distilled water, and H_2-tcpH (31.8 mg, 0.10 mmol) was dissolved in 5 mL of ethanol. Both the solutions were mixed and stirred at room temperature. About 15 min later obtained the homogeneous solution, which was allowed to stand at room temperature for slow evaporation. Three weeks later crystals started to form and the yield was about 53%. These were further washed with ethanol–distilled water (v/v = 1 : 1), and dried in vacuum desiccators. Anal. calcd for $C_{15}H_{10}Cl_4N_2O_5$: C, 40.90; H, 2.27; N, 6.36%. Found: C, 42.45; H, 2.45; N, 7.52%. Infrared spectrum (KBr disc, cm^{-1}): 3435m, 3150, 3075s, 2818m, 2752m, 2569m, 1909s, 1718w, 1622w, 1594m, 1532m, 1451m, 1406m, 1338w, 1265w, 1244w, 1126s, 1108s, 1004s, 921m, 901m,

873m, 816m, 790s, 745w, 720w, 671m, 646m, 618w, 609m, 551m, 467s, 422m, 411m.

X-ray Crystal Structure Analyses

The samples for single crystal diffraction of complexes **1**–**8** were synthesised through the manner described above and selected to be glued at the top of a thin glass fiber with epoxy glue in air for data collection, and the crystallographic data were collected on a Siemens Smart CCD diffractometer equipped with a normal-focus, 2.4 kW sealed-tube X-ray source (graphite-monochromatic MoKa radiation (λ = 0.71073 Å)) operating at 50 kV and 40 mA. There was no evidence of crystal decay during data collection. All crystal structures were solved by direct methods and refined on F^2 by full-matrix least squares methods using the SHELXL program package.[23] Crystallographic details are summarized in **Table 1** and pertinent intermolecular interactions parameters in the structures of **1**–**8** are listed in **Table 2** and **3**.

Results and Discussions

Crystal Structure Analysis of Complex 1. The crystal of **1** crystallizes in the monoclinic system with $P2_1/n$ space group with one molecule of tetrachlorophthalic acid (H_2-tcpH), one tetrachlorophthalic acid anion (H-tcpH$^-$), one 1,10-phen cation and one molecule of methanol in the asymmetric unit in the Figure 1a, and the dihedral angle between the two benzene rings of acid molecules is 4.5°. Within each 1,10-phen component, the dihedral angle between two pyridyl rings is 1.1°, and they make dihedral angles of 1.0° and 0.7°, respectively, with the central benzene ring, revealing the favourable coplanar character. One of the H atoms of the H_2-tcpH acid transfers to one of the N atoms of the 1,10-phen molecule. Analysis of the intermolecular interactions in **1** reveals that the adjacent H_2-tcpH molecules form a one-dimensional (1D) chain *via* the strong hydrogen bonding O–H···O (2.571 and 2.585 Å), which is shown in Figure 1b. In the Figure 1c, the adjacent 1D chains, which are assembled with 1,10-phen and CH_3OH solvent *via* both strong hydrogen bonding O–H···O, N–H···O and weak C–H···O interactions, producing a 2D wavelike structure. In this structure, the solvent molecules are showed in space-filling model in yellow colour. The hydrogen bonding O1–H1···O7 connect the adjacent 2D layers to form the 2D double sheets which is displayed in Figure 1d and is colour coded in yellow. Analysis again suggests that the 2D double layers are connected to form a 3D structure in the *ac* plane by the unique type II Cl···Cl interactions (distance 3.513 Å, θ_1=161.1°, θ_2=122.0°, which is shown in Table 3). Through the Cl5···Cl6 interactions, unique synthons XIX and XX (displayed in scheme 4) can be found in 3D network. To show more clearly, we display the each 2D sheet in different colours, and the solvent molecules are showed in yellow space-filling model. Further analysis of the crystal packing indicates that two –COOH groups in an acid unit connect three adjacent acid molecules to form synthon I $R^4_4(22)$ [O1–H1···O7 and O6–H6···O2]. Additionally, synthon II $R^2_4(18)$ (see in Scheme 3) and synthons XV $R^3_3(14)$, XVI $R^8_8(50)$ (see in supporting information) cannot be neglected, which connect the neighbouring layers and can be found in 3D network.

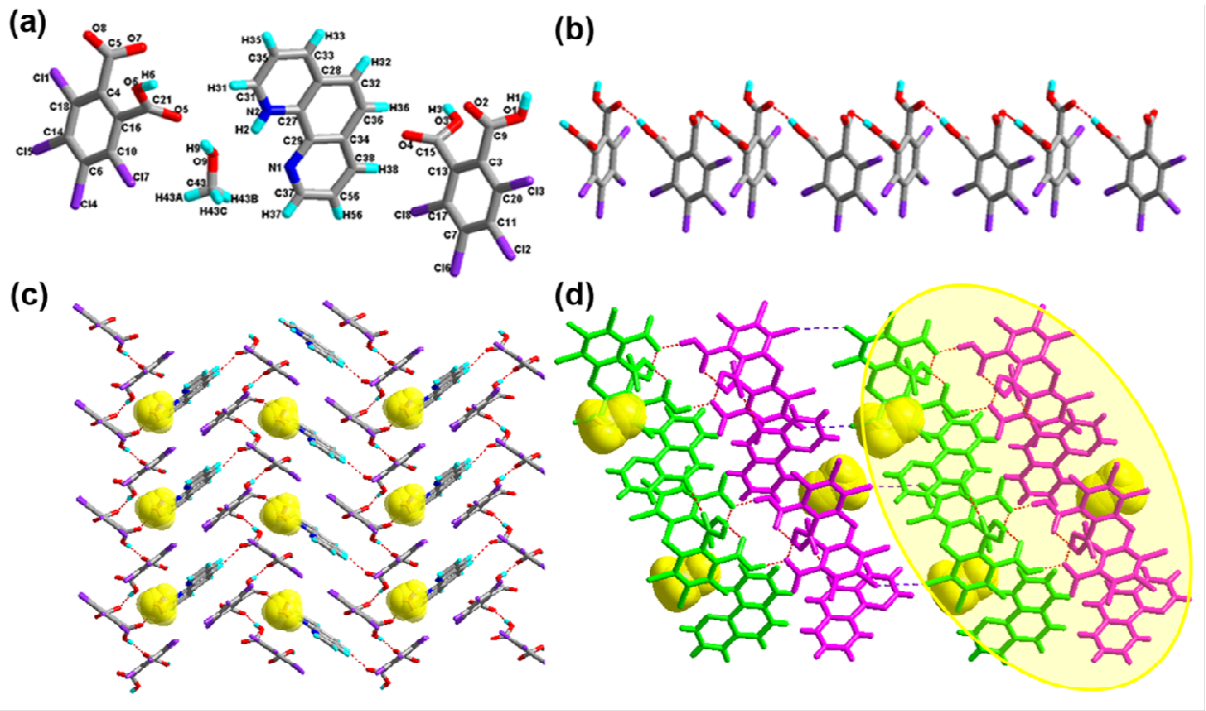

Figure 1. (a) Molecule structure of **1** with atom label of the asymmetric unit; (b) 1D supramolecular chain via hydrogen bonds (the hydrogen bonds are indicated as broken lines in this and the subsequent figures); (c) Perspective view of the 2D hydrogen-bonded layer; (d) 3D network via Cl···Cl interactions, the solvent molecules in this structure are displayed in space-filling model, and the 2D double sheet is colour coded in yellow. (O, red; N, blue; C, gray; H, turquoise; Cl, violet in this and the subsequent figures).

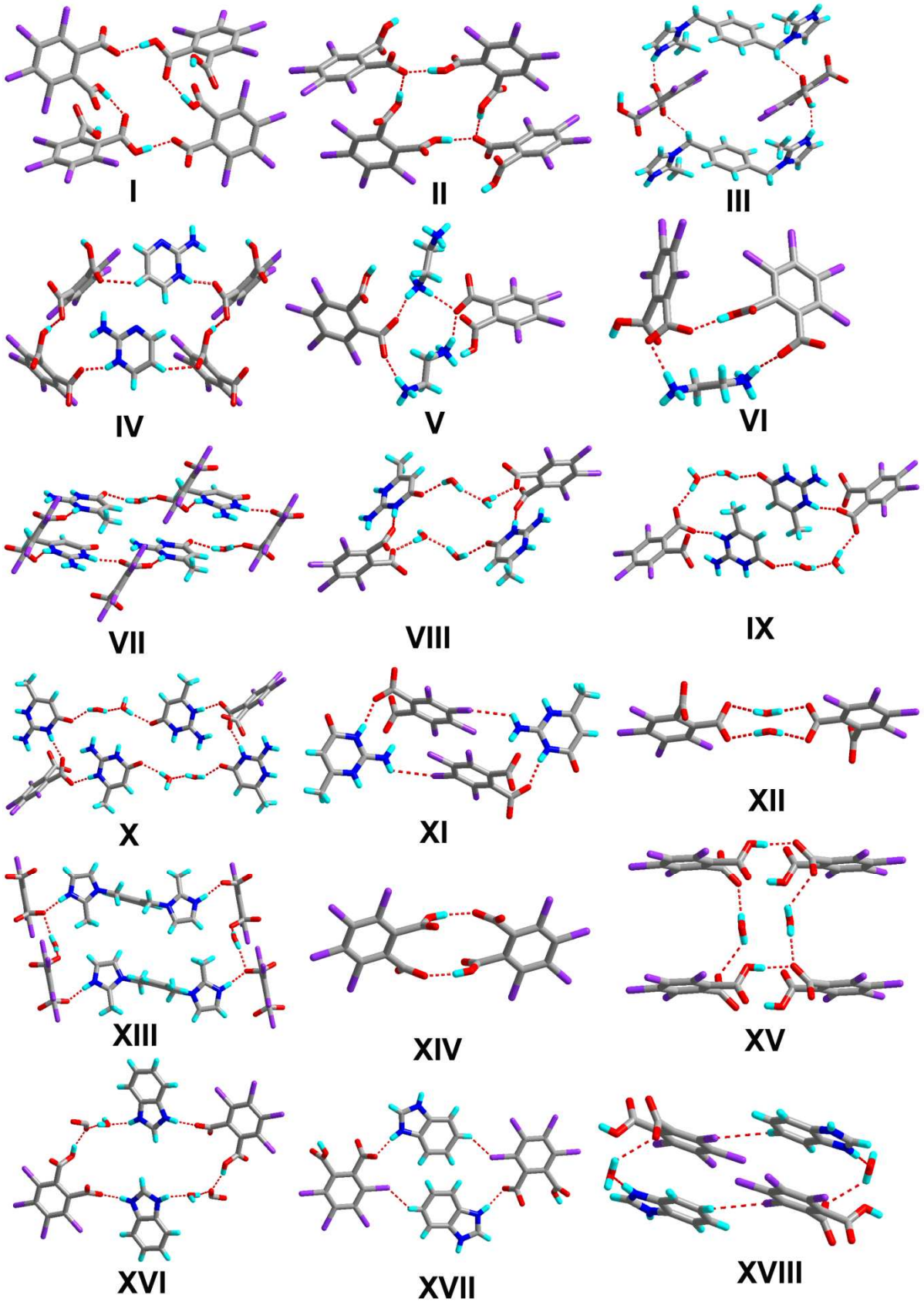

Scheme 3. Supramolecular synthons of complexes 1–8

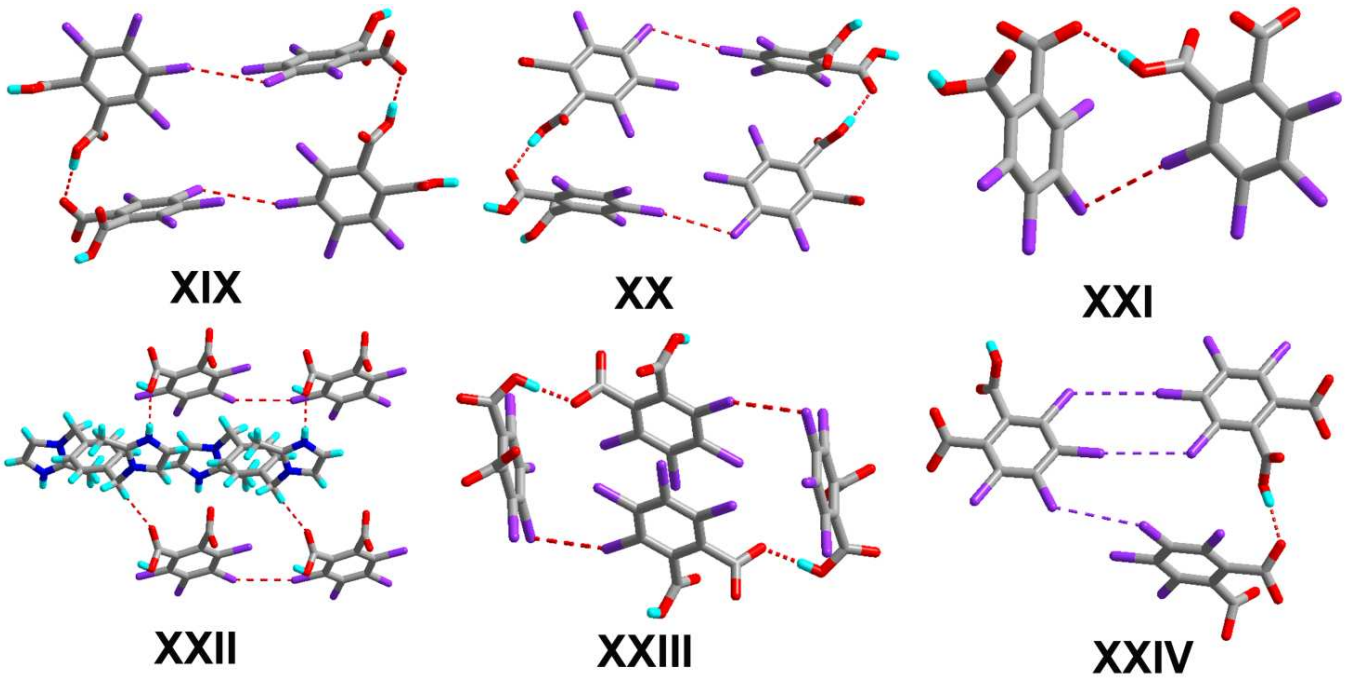

Scheme 4. Synthons (contain Cl···Cl interactions) of complexes 1–5.

Crystal Structure Analysis of Complex 2. The crystal structure of **2** crystallizes in the orthorhombic system with space group *Pbca* (Z=8, in Table 1). As depicted in Figure 2a, the asymmetric unit contains one molecule of H-tcpH$^-$ anion and one of molecule of H-Hatz$^+$ cation. The dihedral angle between triazole ring of Hatz and benzene ring of H_2-tcpH is 71.6°. The amino group and the triazole ring of Hatz are almost in the same plane, and the dihedral angle is 1.3°. In the crystal of **2**, one of the H atoms of the H_2-tcpH acid transfers to N atom of the triazole ring of Hatz. As far as the H_2-tcpH acid components, the adjacent crystallographically independent carboxylic groups are almost vertical to each other. As shown in Figure 2b, the acid molecules arrange each other to exhibit 1D chain *via* the strong hydrogen bonding O3–H3···O2 (2.586 Å) and the base molecules form a 1D chain through the strong hydrogen bonding N1–H1B···N2 (3.058 Å). Through strong N4–H4···O1 interactions, adjacent acid chains and base chains are combined into a 2D sheet, which is displayed in Figure 2c. The adjacent 2D layers connect to form a 2D double layer and we display the 2D double layer colour coded in yellow. Furthermore, the involvement of type II Cl···Cl (Cl3···Cl4 distance 3.280 Å, θ_1=77.7°, θ_2=172.4° and Cl1···Cl2 distance 3.280 Å, θ_1=98.2°, θ_2=144.7°) and strong hydrogen bonding N3–H3A···O2 between 1,2,4-triazole and acid units generate a synthon XXVII $R^6_6(31)$, which is shown in supporting information. As a result, the adjacent 2D layers connect each other to generate 3D network architecture. In this architecture, a unique synthon XXI can be found which contains Cl···Cl interaction. For displayed clearly, we show the 3D network in four colours, and each colour presents a 2D layer in Figure 2d.

Crystal Structure Analysis of Complex 3. The crystal of **3** crystallizes in the triclinic system with space group $P\bar{1}$ with Z=1 (Table 1). There are one H-tcpH$^-$ acid anion and one half H_2-L5$^+$ independent molecule in the asymmetric unit, which is shown in Figure 3a. Within each L5 component, the dihedral angle between the imidazole ring and benzene ring is 89.2°. In the crystal asymmetric unit the dihedral angle is 25.1° between the imidazole ring and the benzene ring of H_2-tcpH acid. Furthermore, the dihedral angle between the benzene rings of L5 and H_2-tcpH is 66.3°. It is notable that H_2-tcpH acid molecules here form intermolecular interactions with L5, including strong N2–H2···O4 hydrogen bonding and strong O1–H1···O1 hydrogen bonding. As shown in the Figure 3b, acid and base subunits arrange alternately to exhibit a 1D chain. Due to the attendance of the hydrogen bonding C21–H21A···O3, these adjacent 1D chains are connected to afford a 2D architecture, which is illustrated in Figure 3c. In this 2D architecture, there are a synthons III $R^4_4(28)$ *via* N2–H2···O4 and C21–H21A···O3 interactions. (in Scheme 2) and a synthon XXVIII $R^6_6(38)$ (in supporting information) *via* N2–H2···O4, C21–H21A···O3 and O1–H121B···O1 interactions. Meanwhile, through type II Cl2···Cl4 interactions (distance 3.399 Å, θ_1=165.8°, θ_2=123.4°), the neighbouring layers are further extended into a 3D cross-link network. In addition, synthon XXII [N2–H2···O4, C21–H21A···O3, Cl2···Cl4] form in this 3D network. For displayed clearly, we show the 2D sheet in different colours in the Figure 3d. Further analysis of the crystal packing suggests that Cl···Cl interactions are very important in expanding the structure dimension.

Crystal Structure Analysis of Complex 4. The complex **4** crystallizes in the monoclinic system with space group $P2_1/c$ (Z=4, in Table 1). In the molecule structure of **4** (Figure 4a), the local asymmetric unit contains two molecules of H-tcpH$^-$ acid anion and two molecules of Hampym$^+$ base cation. Within the unit components the dihedral angle is 77.6° between the two benzene rings, and the

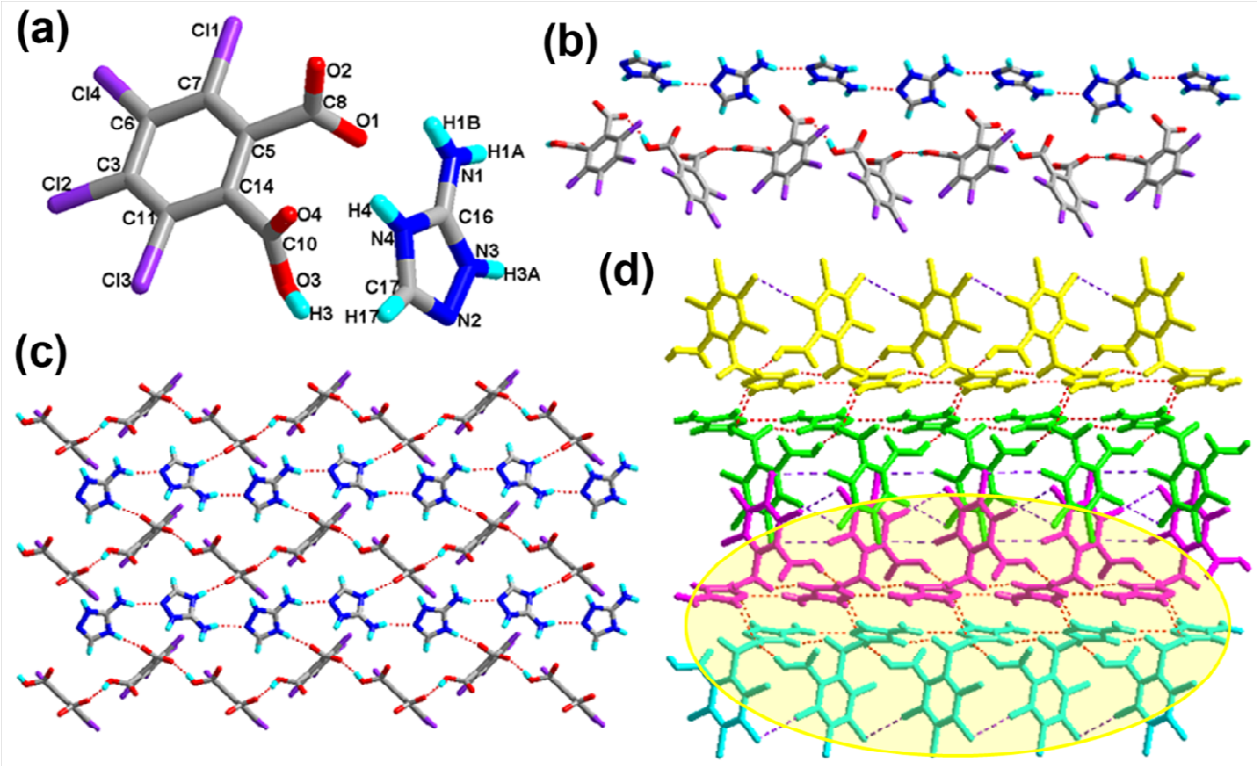

Figure 2. (a) Molecular structure of **2** with atom label of the asymmetric unit; (b) 1D acid chain and base chain via hydrogen bonds; (c) Perspective view of the 2D hydrogen-bonded layer; (d) 3D network via Cl···Cl interactions, and the 2D double sheet is colour coded in yellow.

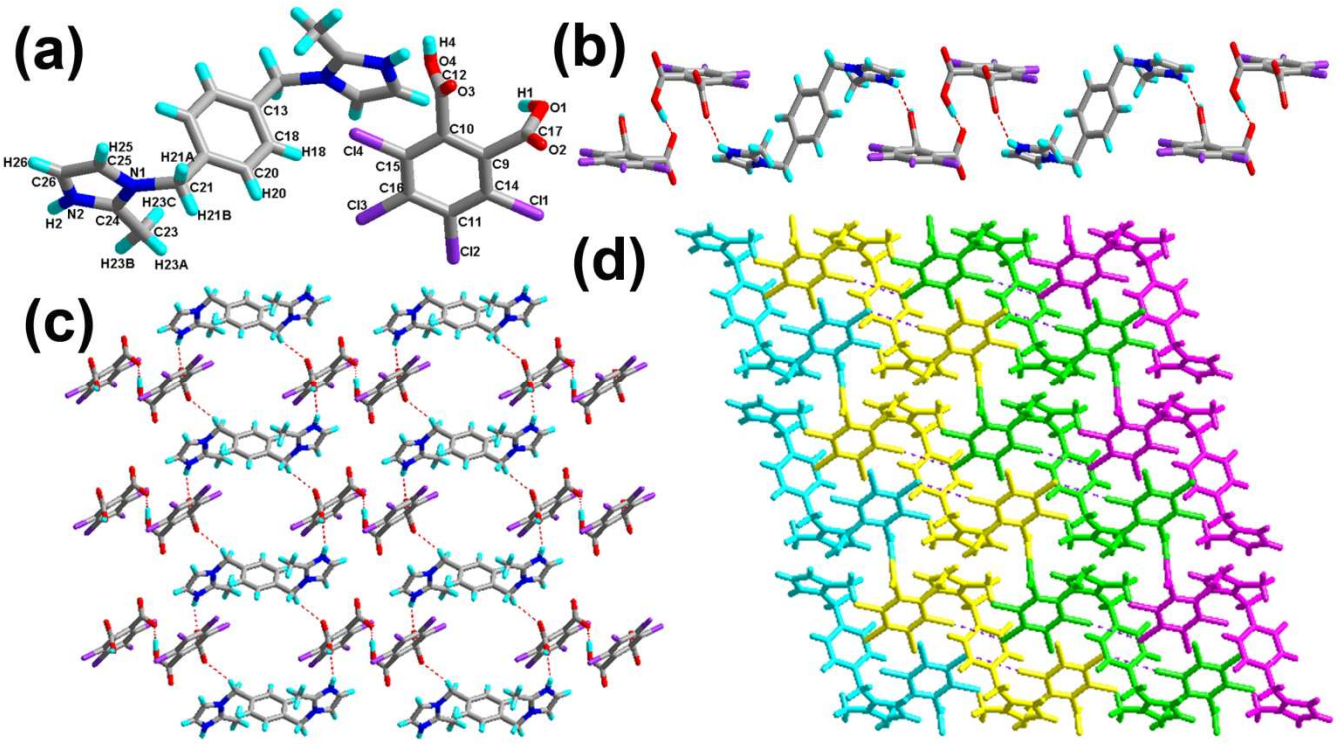

Figure 3. (a) Molecular structure of **3** with atom label of the asymmetric unit; (b) 1D chain via hydrogen bonds; (c) Perspective view of the 2D hydrogen-bonded layer; (d) 3D network via Cl···Cl interactions.

dihedral angle between pyrimidine rings is 37.3°. The dihedral angle between the amino group and pyridine ring is 2.7°. It is notable that the arrangement of carboxylic groups of H_2-tcpH in **4** is different from that in **1**. In crystal of **1** H_2-tcpH molecules and H-tcpH$^-$ acid anion alternately connected to each other, while in the crystal of **4**, the H-tcpH$^-$ acid anion connected to from 1D chains *via* the strong hydrogen bonding O3–H3···O5 in the Figure 4b. Moreover, the carboxylic acid chains join two new patterns of supramolecular synthons IV $R^6_6(30)$, *via* strong N3–H3A···O1, N5–H5···O6, and O8–H8···O2 interactions and weak hydrogen bonding C35–H35···O4 and C38–H38···O7 along the *c* axis to form a 2D layer, which is shown in Figure 4c. The adjacent 2D sheets afford 2D double layer through the hydrogen bonding C35–H35···N1 and C38–H38···N2. Significantly, there is an additional unique type II Cl···Cl interactions (Cl3···Cl4 distance 3.372 Å, θ_1=156.9°, θ_2=95.0° and Cl5···Cl8 distance 3.373 Å, θ_1=94.4°, θ_2=157.0°, shown in Table 3), and as a consequence, 2D double sheets are entangled to build up a unique 3D architecture, which is shown in the Figure 4d and is colour coded in yellow. Additionally, in this network, there is a unique synthon XXIII which is illustrated in scheme 4. This synthon is connected through the Cl···Cl interactions and strong hydrogen bonding O–H···O.

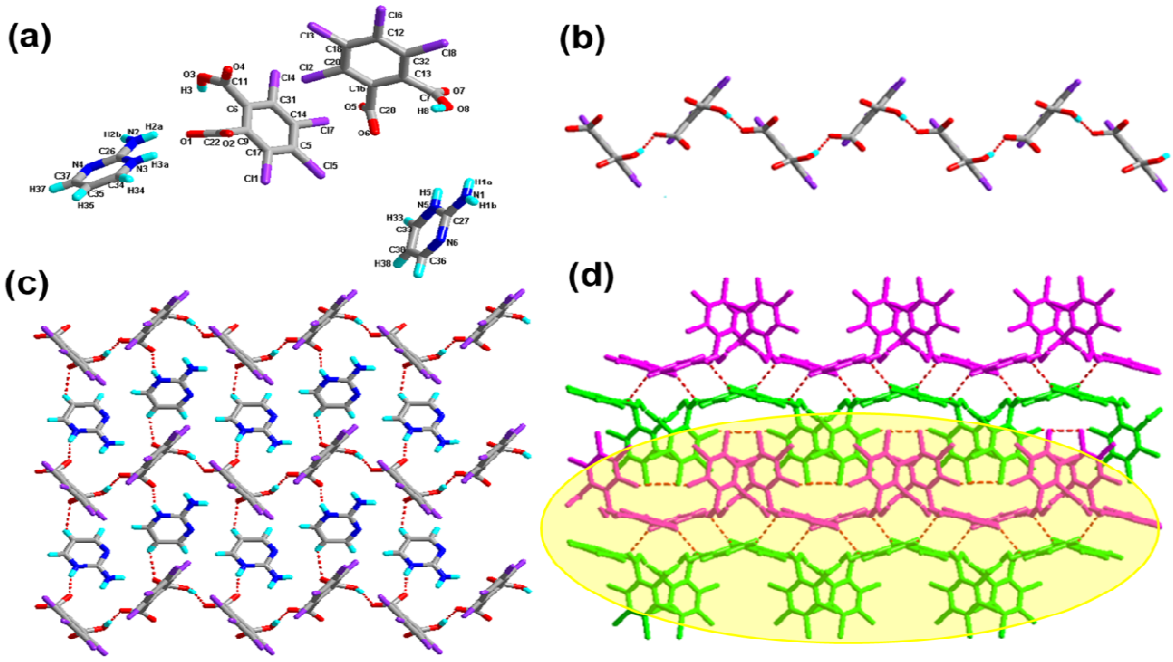

Figure 4. (a) Molecular structure of **4** with atom label of the asymmetric unit; (b) 1D acid chain via hydrogen bonds; (c) Perspective view of the 2D hydrogen-bonded layer; (d) 3D network via Cl···Cl interactions, and the 2D double sheet is colour coded in yellow.

Crystal Structure Analysis of Complex 5. Crystallization of H_2-tcpH acid with edm yields a proton-transfer organic salt **5**, and it crystallizes in the centrosymmetric monoclinic space group *C*2/c with Z=8 (Table 1). The asymmetric unit contains one half H-edm$^+$ cation molecule and one deprotonated H-tcpH$^-$ anion in Figure 5a. In this asymmetric unit, one of the H atoms of H_2-tcpH acid molecules transfers to N atom of edm molecule. Due to the deprotonation effect, it exists usual intramolecular interaction O4–H4···O1 hydrogen bonding to form a 1D chain along *b* axis, which is displayed in Figure 5b. As illustrated in Figure 5c, each H-edm$^+$ cation connects two H-tcpH$^-$ subunits *via* synthon VI $R^3_3(16)$ [O4–H4···O1, N1–H1A···O2 and N1–H1B···O2] and N1–H1C···O1 hydrogen bonding to form a 2D layer. Meanwhile, each H-edm$^+$ molecule is also surrounded by three H-tcpH$^-$ anion subunits and they act as a bridge to the neighbouring 1D chain. In this structure, the adjacent 2D sheets connect to afford 2D double sheets (displayed in Figure 5d and colour coded in yellow) through the hydrogen bonding N1–H1B···O2 (2.847 Å). Due to the N1–H1B···O2 interactions, the 2D double sheets contain a unique synthon V $R^3_4(13)$ (in Scheme 3). Additionally, there are unique type I Cl2···Cl2 (Cl2···Cl2 distance 3.707 Å, θ_1=θ_2=126.8°) and type II Cl3···Cl4 (Cl3···Cl4 distance 3.632 Å, θ_1=122.1°, θ_2=175.4°, which is shown in Table 3) interactions between each H_2-tcpH group. Meanwhile, a unique synthon XXIV Cl_4 [Cl3···Cl4] (scheme 4) can be found in this network, and it is almost identical to the synthon Cl_4 in the article composed by Desiraju.[25] As a consequence, these layers are further extended into a 3D network, which is shown in Figure 5d.

Crystal Structure Analysis of Complex 6. The crystal of **6** crystallizes in the triclinic system with space group *P*$\bar{1}$ (Z=2, in Table 1). The asymmetry unit of **6** (shown in Figure 6a) contains a pair of ahmp$^+$ cation molecules, one tcpH^{2-} dianion molecule, and two water molecules. The two ahmp$^+$ base molecules crystallize with a nearly parallel with the incline angle of only 2.0°. The dihedral angles between pyrimidine ring and benzene ring are 71.8° and 69.8°, respectively. The adjacent acid and base components are linked to form a linear tape *via* N4–H4···O4 (2.668 Å) and N5–H5···O1 (2.774 Å) hydrogen bonding, which is shown in Figure 6b. Both N atoms

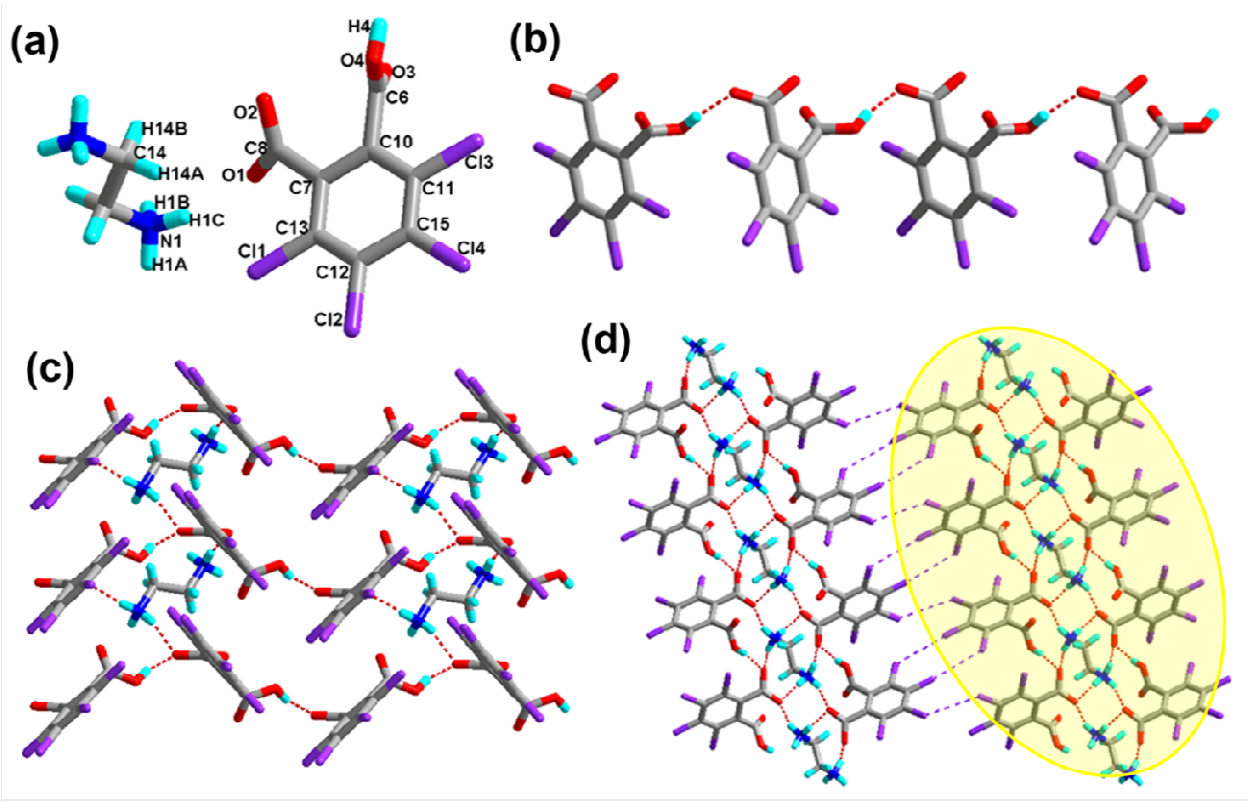

Figure 5. (a) Molecular structure of **5** with atom label of the asymmetric unit; (b) 1D acid chain via hydrogen bonds; (c) Perspective view of the 2D hydrogen-bonded layer; (d) 3D network via Cl···Cl interactions, and the 2D double sheet is colour coded in yellow.

in pyrimidine ring take part in the N4–H4···O4/N5–H5···O1 intermolecular interactions between base and acid units. Meanwhile, as shown in the Figure 6c, one of the water moiety behaves as a hydrogen-bonding 2-connector [O6–H6C···O3 and O6–H6D···O5] with acid and base groups to result in a 2D sheet. In this 2D sheet, there is a larger synthon VII $R^{10}_{10}(46)$, which is shown in Scheme 3. Through further O7–H7A···O8 and O7–H7B···O6 intermolecular interactions, the neighboring 2D layers *via* synthon VIII $R^{8}_{8}(30)$ [N5–H5···O1, O6–H6C···O3, O7–H7B···O6 and O7–H7A···O8], synthon IX $R^{8}_{8}(28)$ [N4–H4···O4, O6–H6C···O3, O7–H7A···O8 and O7–H7B···O6] and synthon X $R^{10}_{10}(36)$ [N1–H1···O2, N5–H5···O1, O6–H6D···O5, O7–H7A···O8 and O7–H7B···O6] to form a 2D double layer, which is displayed in the Figure 6d and is colour coded in yellow in the figure 6e. From another side view, we can clearly see that it is different from the complexes **1**–**5**. In the structure of **6**, it forms N6–H6B···Cl4 hydrogen bonding between the base units and the carboxylic acid units between the adjacent 2D double layers, and thus, result in a 3D architecture, as illustrated in Figure 6e. What's more, a unique synthon XI $R^{4}_{4}(22)$ (in Scheme 3) was obtained, which concludes the weak hydrogen bonding N6–H6B···Cl4. The water moieties in the 3D network are displayed in turquoise colour in space-filling model.

Crystal Structure Analysis of Complex 7. Crystallization of H_2-tcpH acid with L7 yields a proton-transfer organic salt **7**, which crystallizes in the monoclinic system with space group *C*2/*c* (Z=2, in Table 1). The asymmetric unit of **7** consists of one half of the $tcpH^{2-}$ dianion molecule and half of one corresponding monoprotonated L7 dication, as well as two water molecules (see in Fig. 7a). In the cationic moiety, the imidazole ring form dihedral angle of 81.6° with the central benzene ring. The dihedral angle between the benzene ring of the H_2-tcpH acid and the imidazole ring of L7 is 89.1°, and the dihedral angle between two benzene rings is 64.5°. In the structure of **7**, proton transfer from the carboxylic group to imidazole ring of the L7, leading to the formation of charge-assistant N^{+}–H···O^{-} hydrogen bonding. Particularly, the acid and base components display an alternate disposition along [001] direction, that is generated by *b* axis to constitute a distinct 1D chain, which is displayed in the Figure 7b. Notably, one water of H3A–O3–H3B forms a pair of O3–H3A···O1 and O3–H3B···O2 strong hydrogen bonding with the carboxylic groups of the H_2-tcpH acid and the other of N1–H1···O1 hydrogen bonding to define $R^{4}_{4}(12)$ and $R^{6}_{8}(44)$ motifs (synthons XII and XIII shown in scheme 3), which connect the adjacent 1D chains to generate a 2D sheet and the water molecules are showed in space-filling model in bright green colour (see in Fig. 7c). Adjacent layers are further connected through the weak C15–H15···Cl2 interactions between acid and base components, neighbouring sheets are connected to result in a 3D network along the [001] direction in the Figure 7d, and for displaying more clearly, we show the 2D layers in different colours.

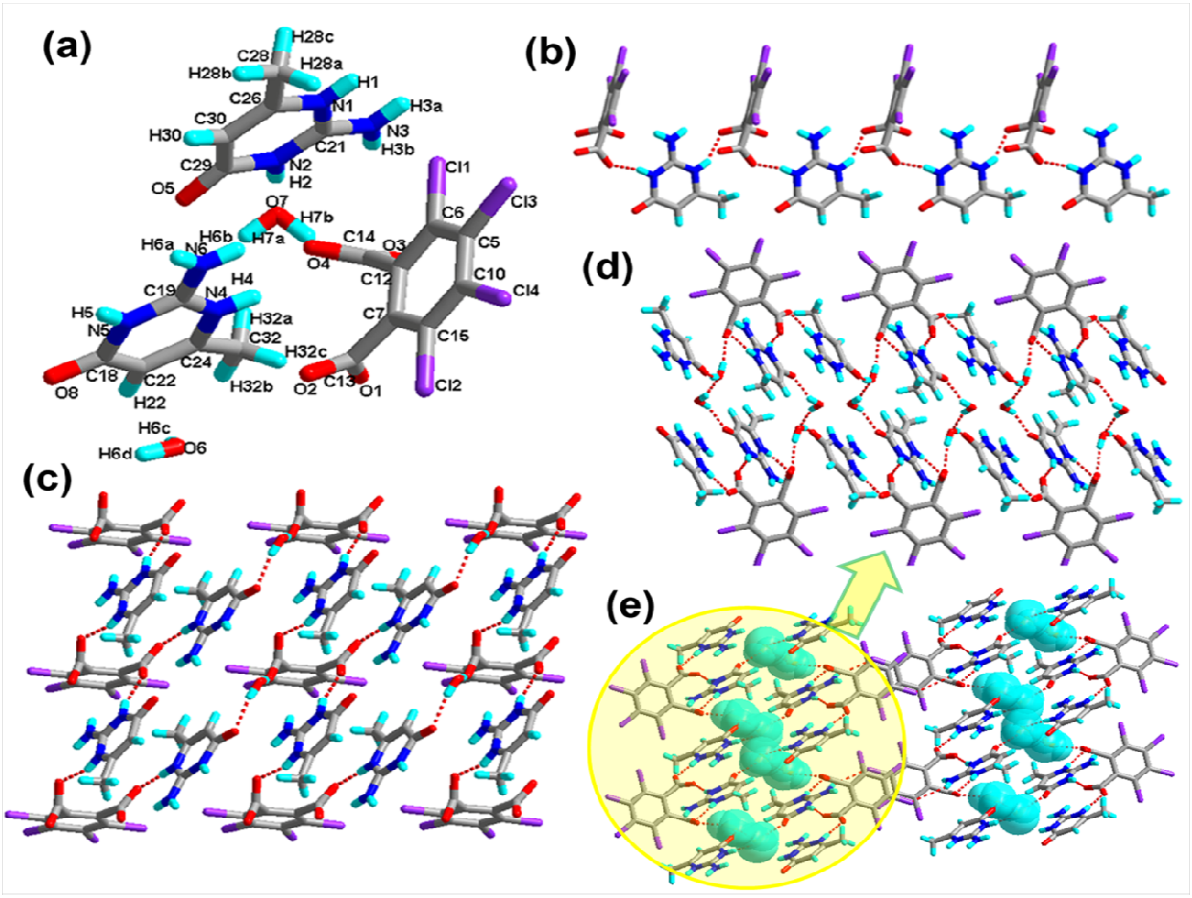

Figure 6. (a) Molecular structure of **6** with atom label of the asymmetric unit; (b) 1D acid chain via hydrogen bonds; (c) Perspective view of the 2D hydrogen-bonded layer; (d) 2D double layer via water molecule; (e) 3D network via N–H···Cl hydrogen bonding, and the 2D double sheet is colour coded in yellow.

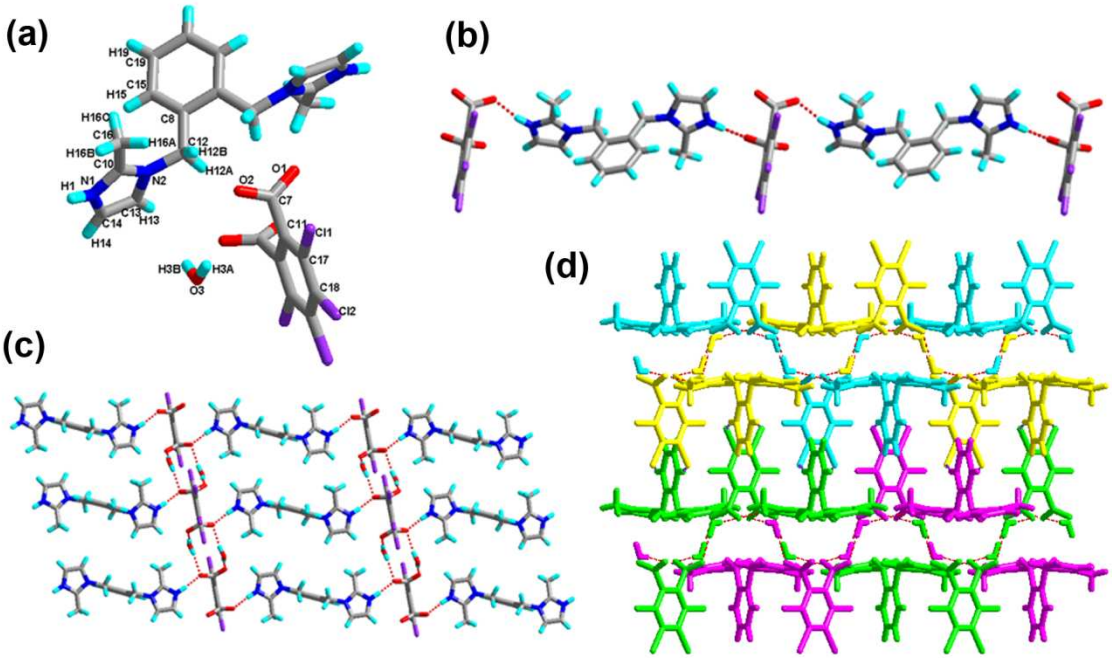

Figure 7. (a) Molecular structure of **7** with atom label of the asymmetric unit; (b) 1D chain via hydrogen bonds; (c) Perspective view of the 2D hydrogen-bonded layer; (d) 3D network via C–H···Cl hydrogen bonding.

Crystal Structure Analysis of Complex 8. The structure of **8** is composed of one H_2-tcpH acid anion, one Bim cation, and two lattice water molecules in the asymmetric unit (see in Figure 8a), and the crystal crystallizes in the triclinic space group $P\bar{1}$ with Z=2 (Table 1). The dihedral angle between the two benzene rings of H_2-tcpH acid and Bim is 29.2°. The imidazole ring of Bim deviates by 0.7° from the benzene ring plane, it is almost coplane. In this case, a unusual chain is produced along *c* axis *via* strong O5–H5A···O2 and O5–H5B···O1 interactions from the water bridges, and which is displayed in the Figure 8b. Furthermore, the H atoms of imidazole ring here lead to the formation of N1–H1···O1 and N2–H2···O5 hydrogen bonding between the water molecule and H_2-tcpH acid moieties from adjacent 1D chains (synthon XXX $R^6_8(24)$ in supporting information), generating a nearly planar 2D supramolecular sheet (see in Figure 8c). Eventually, interlayer O3–H3···O2 hydrogen bonding between the acid molecules extend the 2D patterns to a 2D double layers, and these interactions to define synthons XIV $R^2_2(14)$ [O3–H3···O2], XV $R^6_6(24)$ [O3–H3···O2 O5–H5A···O2 and O5–H5B···O1] and XVI $R^6_8(30)$ [N1–H1···O1, N2–H2···O5, O3–H3···O2 and O5–H5A···O2], whereas the other of the weak hydrogen bonding C19–H19···Cl2, which interlink the 2D double layers to construct a 3D hydrogen-bonded network (see in Figure 8d). Due to the weak hydrogen bonding C19–H19···Cl2, a unique synthon XVII $R^4_4(24)$ (in Scheme 3) appears in 3D architecture.

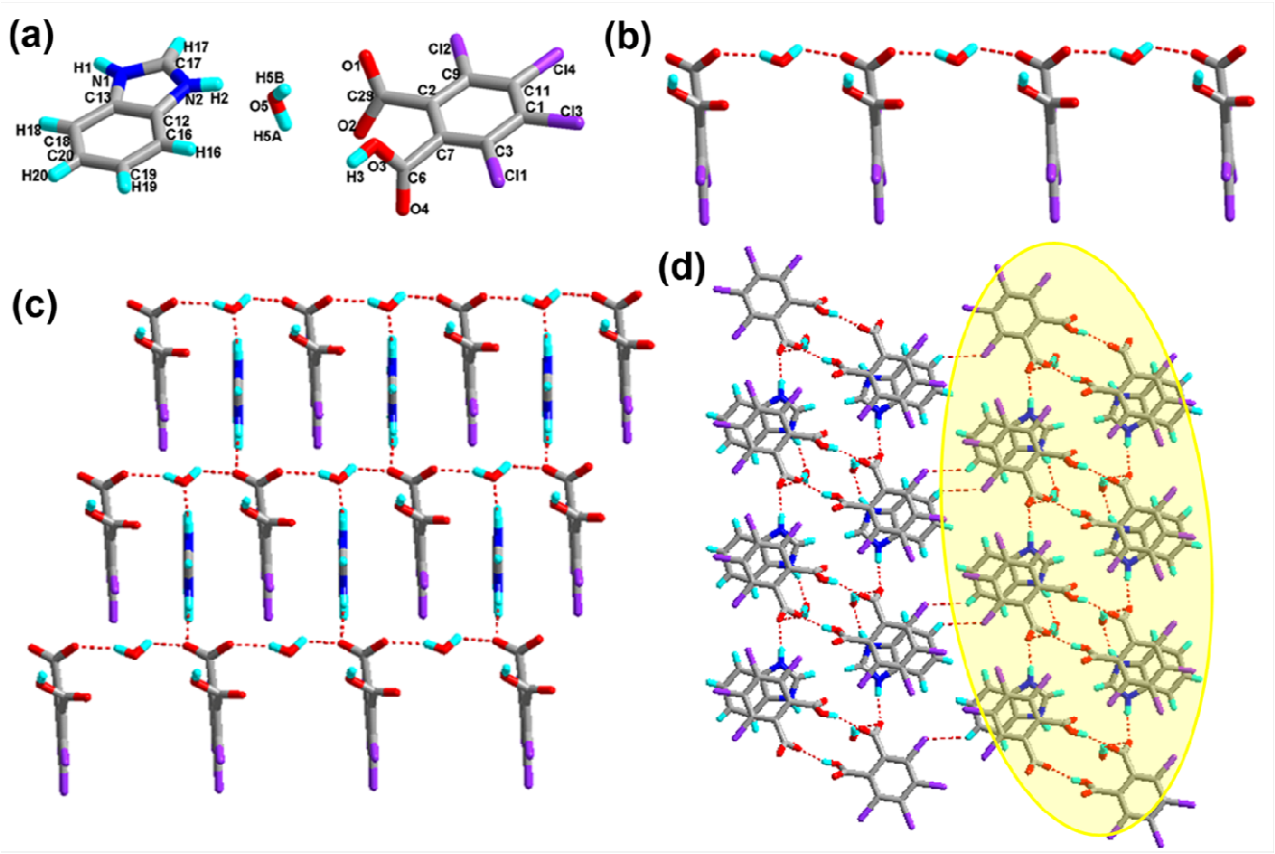

Figure 8. (a) Molecular structure of **8** with atom label of the asymmetric unit; (b) 1D acid chain via hydrogen bonds; (c) Perspective view of the 2D hydrogen-bonded layer; (d) 3D network *via* C–H···Cl hydrogen bonding, and the 2D double sheet is colour coded in yellow.

Thermal stability analysis

All complexes **1–8** are stable in air and can maintain their structural integrity at ambient conditions for a long time. In order to examine the thermal stability of all complexes, the TGA and DSC were carried out between room temperature and 900°C in nitrogen atmosphere. The DSC traces and TGA data for the crystals are presented in Supporting Information. TGA experiments were implemented to investigate their thermal stability. As for complex **3**, the TGA results indicate that they remain intact until 205°C, and then there are a sharp weight loss ending at 280°C (peaks: 265.1°C for crystal **3**). The weight loss of complex 6 up to 60.30% to 260°C corresponds to the loss of acid molecule (calculated: 70.48%). The second weight loss of 39.74% (calculated: 29.53%) can be detected from 280 to 527°C, which is owed to decomposition of base molecule. The TGA curve of **5** is very similar to complex **3**, which indicates the two consecutive weigh losses of acid and base molecules from 135 to 260°C (peaking at 210.18°C) and 310 to 472°C (peaking at 433.53°C). The other two consecutive weight losses are about acid and base components. The TGA curves of **7** and **8** are very similar, which indicate that there are two consecutive weight losses of the two samples. Complex **7** decomposes from 61 to 115°C (peaking at 90.41°C), which corresponds to the water molecules. While in complex **8**, the loss of water continues to 160°C. When it comes to 163°C and 165°C, respectively, the decomposition of the framework begin in the complex **7** and **8** (peaking at 319.4°C and 218.6°C, respectively). As for **1**, the first weight loss of 6.97%

from 78 to 168°C (calculated: 3.90%) corresponds to the loss of one methanol molecule per formula. The second weight loss of 58.86% (calculated: 75.12%) can be detected from 168 to 242°C, which is owed to decomposition of acid molecule, and the second weight loss represented the loss of base components (calculated: 24.15%, found: 36.96%). Compared with complex **1**, the TGA measurement of **2** shows a weight loss of 11.90% in the temperature range 165 to 256°C, which corresponds to the loss of 3-amino-1,2,4-triazole molecule, and the second weight loss represented the loss of acid components (calculated: 79.38%, found: 66.55%). The TGA measurement of **4** indicates that the complex does not melt and is stable up to 166°C, at which temperature the crystal begins to decompose. The ligand benzimidazole decomposes at 166 to 178°C (peaking at 165.18°C), the second weight loss of 85.55% from 178 to 380°C, which corresponds to the acid molecules. Moreover, the theoretical value and practical value differ within a reasonable range. Broadly speaking, the eight frameworks have a remarkably thermal stability.

Conclusions

In this article, we have successfully synthesized and characterized eight new complexes by using H_2-tcpH acid ligand along with a series of N–heterocyclic compounds. X-ray analysis revealed that these salts exhibit different intriguing architectures in which various hydrogen bonding and halogen···halogen interactions are found as well. All of the eight complexes have the H_2-tcpH acid molecule, and the H atom of carboxylate group transfer to the base molecule. Furthermore, structural analysis of complexes **1**–**8** found that only one H atom transfers in complexes **1**–**5** and **8**, while the proton transfer occurs entirely in complexes **6** and **7**. Different from the other crystals, the complex **1** contains a methanol solvent molecule in asymmetry unit. More than that, the complexes **1**–**8** display intriguing 3D structures, what is more, they form a 2D double layer by the different hydrogen bonding, expect the complex **5**. In addition, it is nice to note that in crystals **1**–**5**, they demonstrate 3D architectures *via* Cl···Cl interactions, while in complexes **7**–**8** the adjacent 2D organic layers are further connected through the weak hydrogen bonding C–H···Cl, generating a 3D network. According to the above structural description of our complexes, we find that H_2-tcpH acid ligand adopts a variety of connected modes, and it is a good candidate for constructing supramolecular.

Moreover, in all of these 3D supramolecular complexes the strong hydrogen bonding O–H···O, N–H···O, N–H···N, and the weak C–H···O, C–H···Cl, N–H···Cl, Cl···Cl interactions are present. They not only extend these networks from 1D to 2D/3D, but also reinforce their structures because of the synthons formed by these interactions are stable in complexes **1**–**8**. The weak hydrogen bonding C–H···O can affect the crystal packing in unpredictable ways, and it used widely in crystal engineering to construct synthons as addressed in previous accounts.[24] In complex **3**, C–H···O hydrogen bonding participate in the synthon formation in III and XXII. Due to the stereochemistry effect, the classical synthons $R^2_2(6)$ and $R^2_2(8)$ have not been found in complexes **1**–**8**. Nevertheless, a number of larger synthons exist in these structures, for example, synthons III, IV, VII, X, XIII, XVI, XVII and XX. Clearly, the presence of the H_2-tcpH acid is a common structural feature of these larger synthons, and it is obvious that the "supramolecular synthon" strategy will be frequently applied in designing novel periodic and predictable superstructures.

Acknowledgements

This work was financially supported by the National Natural Science Foundation of China (No. 51372125, 21371105, and 21203106), and the Scientific and Technical Development Project of Qingdao (No. 13-1-4-184-jch).

Reference

1. (a) T. R. Cook, Y. R. Zheng and P. J. Stang, *Chem. Rev.*, 2013, **113**, 734−777; (b) M. M. Conn and J. Rebek, *Jr. Chem. Rev.*, 1997, **97**, 1647−1668; (c) A. Jasat and J. C. Sherman, *Chem. Rev.*, 1999, **99**, 931−967; (d) S. S. Mondal, A. Bhunia, A. Kelling, U. Schilde, C. Janiak and H. J. Holdt, *J. Am. Chem. Soc.*, 2014, **136**, 44−47; (e) R. Chakrabarty, P. S. Mukherjee and P. J. Stang, *Chem. Rev.*, 2011, **111**, 6810–6918; (f) G. A. Hembury, V. V. Borovkov and Y. Inoie, *Chem. Rev.*, 2008, **108**, 1−73; (g) B. Bibal, C. Mongin and D. M. Bassani, *Chem. Soc. Rev.*, 2014, **43**, 4179−4198; (h) L. Wang, L. Zhao, L. Y. Xu, R. X. Chen and Y. Yang, *CrystEngComm*, 2012, **14**, 6998−7008; (i) L. Wang, L. Zhao, Y. J. Hu, W. Q. Wang, R. X. Chen and Y. Yang, *CrystEngComm*, 2013, **15**, 2835−2852; (j) L. Wang, L. Zhao, W. M. Liu, R. X. Chen, Y. X. Gu and Y. Yng, *Sci. China Chem*., 2012, **55**, 2381−2387.
2. (a) K. Biradha, A. Nangia, G. R. Desiraju, C. J. Carrell and H. L. Carrell, *J. Mater. Chem.*, 1997, **7**, 1111–1122; (b) V. R. Thalladi, H. C. Weiss, D. Bläser and R. Boese, *J. Am. Chem. Soc*., 1998, **120**, 8702−8710; (c) S. R. Perumalla, V. R. Pedireddi and C. C. Sun, *Mol. Pharmaceutics*, 2013, **10**, 2462−2466; (d) L. Wang, L. Zhao, M. Liu, F. Q. Liu, R. X. Chen, Y. Yang and Y. X. Gu, *Sci. China Chem*., 2012, **55**, 2115−2122.
3. (a) M. Pérez-Torralba, M. Ángeles García, C. López, M. C. Torralba, M. R. Torres, R. M. Claramunt and J. Elguero, *Cryst. Growth Des*., 2014, **14**, 3499−3509; (b) G. Nandi, H. M. Titi and I. Goldberg, *Cryst. Growth Des*., 2014, **14**, 3557−3566; (c) P. Panini and D. Chopra, *Cryst. Growth Des.*, 2014, **14**, 3155−3168; (d) F. Bertolotti, A. V. Shishkina, A. Forni, G. Gervasio, A. I. Stash and V. G. Tsirelson, *Cryst. Growth Des.*, 2014, **14**, 3587−3595; (e) E. Guzamán-Percástegui, J. G. Alvarado-Rodríguez, J. Cruz-Borbolla, N. Andrade-López, R. A. Vázquez-Garacía, R. N. Nav-Galindo and T. Pandiyan, *Cryst. Growth Des*., 2014, **14**, 3742−3757.
4. (a) P. Metrangolo, H. Neukorch, T. Pilati and G. Resnti, *Acc. Chem. Res*., 2005, **38**, 386−395; (b) M. Erdélyi, *Chem. Soc. Rev.*, 2012, **41**, 3547–3557; (c) H. R. Khavasi and A. A. Tehrani, *CrystEngComm*, 2013, **15**, 5813–5820; (d) P. Metrangolo, F. Meyer, T. Pilati, G. Resnati and G. Terraneo, *Angew. Chem. Int. Ed*., 2008, **47**, 6114–6127; (e) H. Y. Gao, X. R. Zhao, H. Wang, X. Pang and W. J. Jin, *Cryst. Growth Des.*, 2012, **12**, 4377−4387.

5. (a) J. P. M. Lommerse, A. J. Stone, R. Taylor and F. H. Allen, *J. Am. Chem. Soc.*, 1996, **118**, 3108−3116; (b) M. Freytag, P. G. Jones, B. Ahrens and A. K. Fischer, *New J. Chem.*, 1999, **23**, 1137−1139.
6. (a) M. Podsiadţo, A. O;ejniczak and A. Katrusiak, *CrystEngComm*, 2014, **16**, 8279–8285; (b) R. B. K. Siram, D. P. Karothu, T. N. Guru Row and S. Patil, *Cryst. Growth Des*., 2013, **13**, 1045−1049.
7. (a) M. Baldrighi, G. Cavallo, M. R. Chierotti, R. Gobetto, P. Metrangolo, T. Pilati, G. Resnati and G. Terraneo, *Mol. Pharmaceutics*., 2013, **10**, 1760−1772; (b) R. J. Baker, P. E. Colavita, D. M. Murphy, J. A. Platts and J. D. Wallis, *J. Phys. Chem. A*, 2012, **116**, 1435–1444; (c) V. R. Hathwar, T. S. Thakur, R. Dubey, M. S. Pavan, T. N. Guru Row and G. R. Desiraju, *J. Phys. Chem. A*, 2011, **115**, 12852−12863; (d) D. Chopra, T. S. Cameron, J. D. Ferrara and T. N. Guru Row, *J. Phys. Chem. A*, 2006, **110**, 10465−10477; (e) C. F. Matta, N. Castillo and R. J. Boyd, *J. Phys. Chem. A*, 2005, **109**, 3669–3681; (f) V. R. Hathwar and T. N. Guru Row, *Cryst. Growth Des*., 2011, **11**, 1338–1346; (g) T. Shirman, J. Lamere, L. J. M. Shimon, T. Gupta, J. M. L. Martin and van der Boom, *Cryst. Growth Des*., 2008, **8**, 3066–3072; (h) S. K. Nayak, M. K. Reddy, T. N. Guru Row and D. Chopra, *Cryst. Growth Des*., 2011, **11**, 1578–1596; (i) P. Politzer and J. S. Murray, *ChemPhysChem*, 2013, **14**, 278–294.
8. V. S. Senthil Kumar, F. C. Pigge and N. P. Rath, *CrystEngComm*, 2004, **6**, 102–105.
9. H. Wang, R. X. Hu, X. Pang, H. Y. Gao and W. J. Jin, *CrystEngComm*, 2014, **16**, 7942–7948.
10. (a) M. Li, D. Li, M. O'Keeffe and O. M. Yaghi, *Chem. Rev*., 2014, **114**, 1343−1370; (b) T. Samanta, L. Dey, J. Dinda, S. K. Chattopadyhyay and S. K. Seth, *Journal of Molecular Structure*, 2014, 1068, 58–70; (c) A. Zawada, R. W. Góra, M. M. Mikolajczyk and W. Bartkowiak, *J. Phys. Chem. A*, 2012, **116**, 4409−4416.
11. (a) F. H. Allen, W. D. Samuel Motherwell, P. R. Raithby, G. P. Shields and R. Taylor, *New J. Chem*., 1999, **23**, 25−34; (b) V. R. Thalladi, B. S. Goud, V. J. Hoy, F. H. Allen, J. A. K. Howard and G. R. Desiraju, *Chem. Commun.*, 1996, **3**, 401−402.
12. (a) G. R. Desiraju, *Angew. Chem. Int. Ed. Engl*., 1995, **34**, 2311-2327; (b) S. Tothadi and G. R. Desiraju, *Chem. Commun.*, 2013, **49**, 7791–7793; (c) A. Mukherjee, S. Tothadi, S. Chakraborty, S. Ganguly and G. R. Desiraju, *CrystEngComm*, 2013, **15**, 4640–4654; (d) M. Du, Z. H. Zhang and X. J. Zhao, *Cryst. Growth Des*., 2011, **11**, 1199–1208; (e) M. Du, Z. H. Zhang and X. J. Zhao, *Cryst. Growth Des*., 2005, **5**, 1247–120854; (f) M. Du, Z. H. Zhang, X. J. Zhao and H. Cai, *Cryst. Growth Des*., 2006, **6**, 114–121; (g) M. Du, X. J. Jiang, X. Tan, Z. H. Zhang and H. Cai, *CrystEngComm*, 2005, **5**, 454–462; (h) S. Tothadi, A. Mukherjee and G. R. Desiraju, *Chem. Commun*., 2011, **47**, 12080–12082.
13. K. Merz, M. V. Evers, F. Uhl, R. I. Zubatyuk and O. V. Shishkin, *Cryst. Growth Des.*, 2014, **14**, 3124−3130.
14. H. R. Khavasi and M. Esmaeili, *CrystEngComm*, 2014, 16, 8479–8485.
15. C. Zhang, Z. Yang, X. Q. Zhou, C. H. Zhang. Y. Ma, J. J. Xu, Q. Zhang, F. Nie and H. Z. Li, *Cryst. Growth Des.*, 2014, **14**, 3923−3928.
16. (a) J. A. R. P. Sarma, F. H. Allen, V. J. Hoy, J. A. K. Howard, R. Thaimattam, K. Biradha and G. R. Desiraju, *Chem. Commun*., 1997, 101−102; (b) K. S. Eccles, R. E. Morrison, A. R. Maguire and S. E. Lawrence, *Cryst. Growth Des*., 2014, **14**, 2753−2762; (c) A. Mukherjee and G. R. Desirju, *Chem. Commun*., 2011, **47**, 4090–4092; (d) V. R. Thalladi, S. Brasselet, D. Bläser, R. Boese, J. Zyss, A. Nangia and G. R. Desiraju, *Chem. Commun.*, 1997, **19**, 1841−1842.
17. (a) P. J. Langley, J. Hulliger, R. Thaimattam and G. R. Desiraju, *New J. Chem.*, 1998, 22, 1307−1309; (b) S. R. Perumalla, E. Suresh and V. R. Pedireddi, *Angew. Chem. Int. Ed.*, 2005, **44**, 7752–7757; (c) V. R. Vangala, R. Mondal, C. K. Broder, J. A. K. Howard and G. R. Desiraju, *Cryst. Growth Des*., 2005, **5**, 99−104.
18. (a) S. Kumaresam, P. G. Seethalakshmi, P. Kumaradhas and B. Devipriya, *Journal of Molecular Structure*, 2013, **1032**, 169–175; (b) S. W. Jin, M. Guo, D. Q. Wang and H. Cui, *Journal of Molecular Structure*, 2011, **1006**, 128–135; (c) L. Wang, W. Y. Xu, Y. J. Hu, Y. Y. Pang, F. Q. Liu and Y. Yang, *RSC Adv.*, DOI: 10.1039/C4RA08452G; (d) L. Wang, L. Zhao, M. Liu, R. X. Chen, Y. Yang and Y. X. Gu, *Sci. China Chem*., 2012, **55**, 2115−2122; (e) L. Wang, R. Y. Xue, Y. X. Li, Y. R. Zhao, F. Q. Liu and K. K. Huang, *CrystEngComm*., 2014, **16**, 7074–7089.
19. (a) A. Muhherjee and G. R. Desiraju, *Cryst. Growth Des.*, 2014, **14**, 1375−1385; (b) S. Tothadi, S. Joseph and G. R. Desiraju, *Cryst. Growth Des*., 2013, **13**, 3242−3254; (c) Y. B. He, S. C. Xiang and B. L. Chen, *J. Am. Chem. Soc*., 2011, **133**, 14570–14573; (d) P. K. Knacharla, T. Kato and D. Crich, *J. Am. Chem. Soc*., 2014, **136**, 5472−5480; (e) P. Li, Y. B. He, H. D. Arman, R. Krishna, H. L. Wang, L. H. Weng and B. L. Chen, *Chem. C ommun*., 2014, **50**, 13081−13084; (f) F. Guo, F. Wang, H. Yang, X. L. Zhang and J. Zhang, *Inorg. Chem*., 2012, **51**, 9677−9682.
20. (a) F. Zordan, L. Brammer and P. Sherwood, *J. Am. Chem. Soc*., 2005, **127**, 5979–5989; (b) S. K. Nayak, M. K. Reddy, T. N. Guru Row and D. Chopra, *Cryst. Growth Des*., 2011, **11**, 1578–1596.
21. (a) L. Wang, L. Zhao, Y. J. Hu, W. Q. Wang, R. X. Chen and Y. Yang, *CrystEngComm*, 2013, **15**, 2835–2852; (b) L. Wang, Y. J. Hu, W. Q. Wang, F. Q. Liu and K. K. Huang, *CrystEngComm*, 2014, **16**, 4142–4161.
22. B. F. Hoskins, R. Robson and D. A. Slizys, *J. Am. Chem. Soc.*, 1997, **119**, 2952–2953.
23. (a) G. M. Sheldrick, SHELXS-97, Program for the Solution of Crystal Structures, University of Göttingen, Göttingen, Germany, 1997; (b) G. M. Sheldrick, SHELXL-97, Programs for X-ray Crystal Structure Refinement, University of Göttingen, Göttingen, Germany, 1997.
24. (a) T. Steiner, *New J. Chem*., 1998, **22**, 1099–1103; (b) P. K. Thallapally, A. K. Katz, H. L. Carrell and G. R. Desiraju, *CrystEngComm*, 2003, **5**, 87–92; (c) N. N. Laxmi Madhavi, C. Bilton, J. A. K. Howard, F. H. Allen, A. Nangia and G. R.

Desiraju, *New J. Chem*., 2000, **24**, 1–4; (d) R. Thaimattam, D. S. Reddy, F. Xue, T. C. W. Mak, A. Nangia and G. R. Desiraju, *J. Chem. Soc., Perkin Trans.*, 1998, **2**, 1783–1789.

25. R. Banerjee, G. R. Desiraju, R. Mondal, A. S. Batsanov, C. K. Broder and J. A. K. Howard, *Helvertiva Chimica Acta*, 2003, **86**, 1339–1351.

Table of contents

Using Halogen···Halogen Interactions or C/N–H···Cl Hydrogen Bonding to Direct Crystal Packing in Tetrachlorophthalic Acid with N–heterocyclic Compounds

Yanjing Hu, Zhiqiang Li, Yiran Zhao, Yu Yang*,Faqian Liu, and Lei Wang*

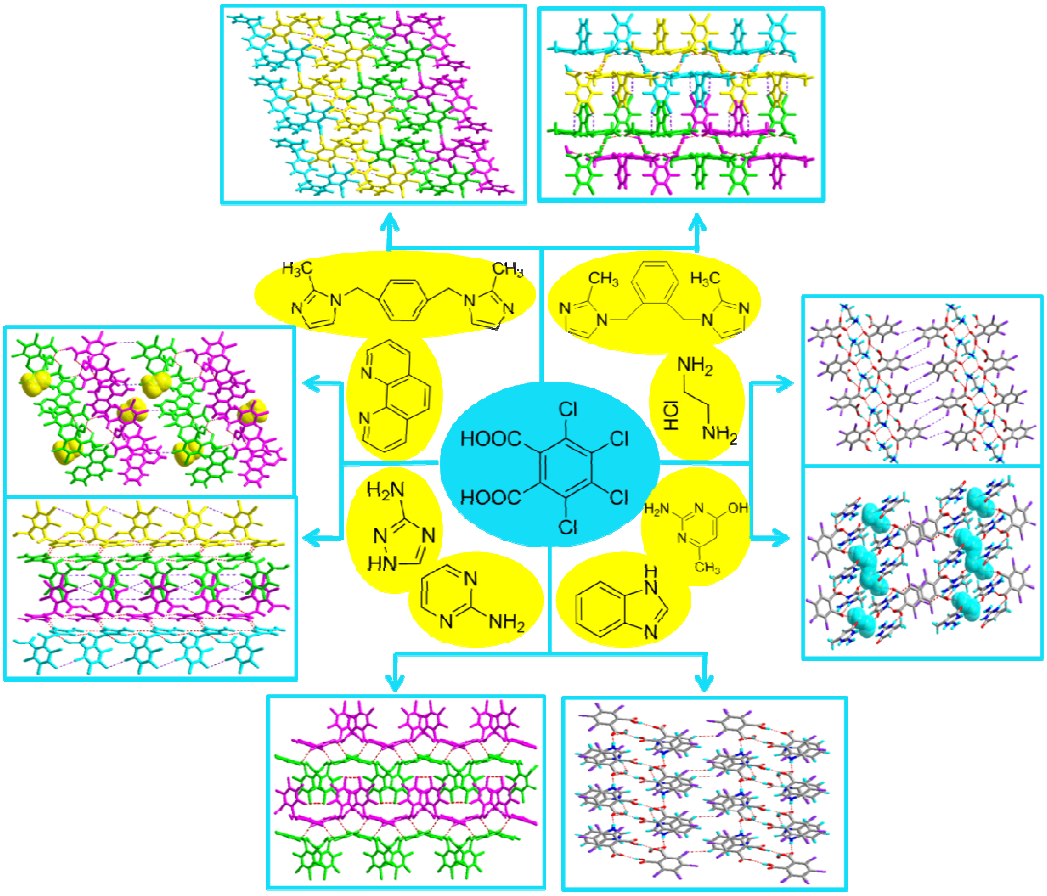

Hydrogen bonding patterns and halogen···halogen interactions, C/N–H···Cl hydrogen bonding in a series of multi-component molecular constructed by tetrachlorophthalic acid with N-heterocycles were discussed in the context.